Physics Letters A 379 (2015) 916–922

Contents lists available at ScienceDirect

Physics Letters A

www.elsevier.com/locate/pla

Theoretical study of energy band splitting induced by spin–orbit interaction in helically coiled carbon nanotubes

Ning Ma [a,b,*], Shengli Zhang [b,*], Vei Wang [c], Daqing Liu [d]

[a] Department of Physics, MOE Key Laboratory of Advanced Transducers and Intelligent Control System, Taiyuan University of Technology, Taiyuan 030024, China
[b] Department of Applied Physics, Xi'an Jiaotong University, Xi'an 710049, China
[c] Department of Applied Physics, Xi'an University of Technology, Xi'an 710054, China
[d] School of Mathematics and Physics, Changzhou University, Changzhou 213164, China

ARTICLE INFO

Article history:
Received 30 September 2014
Received in revised form 23 December 2014
Accepted 16 January 2015
Available online 20 January 2015
Communicated by R. Wu

Keywords:
Spin splitting
Spin–orbit interaction
Carbon nanotubes

ABSTRACT

Recent theoretical and experimental works on straight carbon nanotubes (SCNTs) have revealed that the curvature could enhance the spin–orbit interaction (SOI). Motivated by this, we further explore the effective SOI with another different curvature in helically coiled carbon nanotubes (HCCNTs) using the tight-binding model and perturbation approach. Finally, we derive the effective SOI in HCCNTs, and find the electron–hole asymmetric spin splitting. Interestingly, the asymmetric splitting largely depends on coil pitch p and coil radius r, which are not known in SCNTs. These results should be valuable for spintronic applications of carbon nanotubes.

1. Introduction

Graphene (or a graphite monolayer) is a rapidly rising star on the horizon of materials science and condensed-matter physics [1–4]. Such two-dimensional (2D) or quasi-two-dimensional material exhibits exceptionally high crystal and electronic quality, and, despite its short history, has already revealed a cornucopia of new physics and potential applications [5–13]. Furthermore, it can be rolled into 1D carbon nanotubes (CNTs), which has been gradually regarded as one of the most promising research fields [14–16], owing to their application as building blocks in spintronics [17–20]. Nonetheless, the spin–orbit interaction (SOI) in CNTs has been customarily underestimated [21], due to the low atomic number of carbon ($Z = 6$). Only recently was it proven experimentally [22] that the energy shifts caused by the SOI on ultraclean CNTs are in order-of-magnitude agreement with the theoretical results [23–25], which argued that the curvature could enhance the effective SOI strength. Specifically, the first calculations by Ando [23], later refined by Chico et al. [24] and Huertas-Hernando et al. [25], considered the modification of hopping amplitudes by atomic SOI which gives rise to the orbital-like contribution. But these previous theories cannot explain the chirality dependence of SOI and the considerable asymmetry spin splitting between conduction and valence bands in [22]. Aiming at this problem, Izumida et al. [26] and Jeong et al. [27] further calculate the spin–orbit correction in more detail using tight-binding (TB) method, and find the Zeeman-like contribution to the SOI, thereby giving an explanation for the electron–hole asymmetry splitting. Understanding these effects is essential for the successful manipulation of the different degrees of freedom of these systems, thereby affecting the transport properties of electrons. To date, the spin manipulation via SOI has been extensively studied in straight carbon nanotubes (SCNTs) [28–41].

Motivated by this, we further study the SOI involving a different curvature in helically coiled carbon nanotubes (HCCNTs) that were firstly predicted by Ihara et al. [42], and then founded in experiment [43]. Owing to their potential applications for nano-electronic/nano-electromechanical devices, the HCCNTs have been attracting extensive interest [44–46] in the past years. Regrettably, these researches have just focused on the electronic properties without considering the spintronic properties. Especially, the law of additional SOI induced by the distortion of HCCNTs and its influence on the movement of electrons, remain poorly understood even now. Besides the chirality, how to affect the SOI in HCCNTs? Does the SOI revised by the parameters (i.e. coil pitch p and coil radius r, etc.) have any of the new physical effect? These questions have important academic significance towards designing of new mesoscopic spin electronic devices.

Employing the perturbation theory and the TB method, we finally derive the effective SOI, and find the electron–hole asymmetric spin splitting in HCCNTs, which is attributed to the combined

* Corresponding authors.
E-mail addresses: maning@stu.xjtu.edu.cn (N. Ma), zhangsl@mail.xjtu.edu.cn (S. Zhang).

http://dx.doi.org/10.1016/j.physleta.2015.01.010
0375-9601/

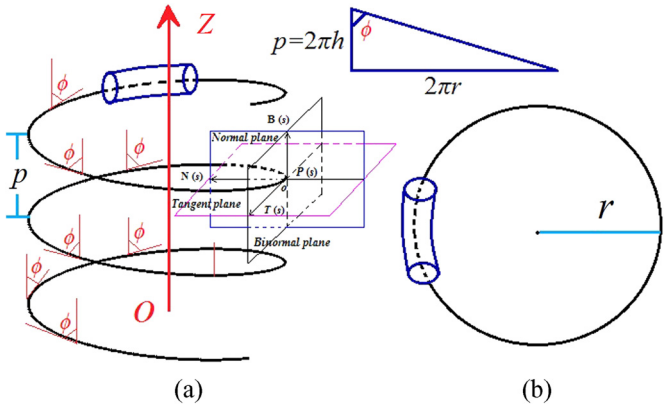

Fig. 1. (Color online.) Schematic of the relevant parameters of HCCNTs with (a) side view and (b) top view.

Table 1
Summary of relevant parameters for a HCCNT.

Name	Symbol
Coil pitch	$p = 2\pi h$
Coil radius	r
Inclination angle of helix	$\phi = \arctan\frac{r}{h}$
Curvature of $\boldsymbol{P}(s)$	$\kappa(s) = \frac{r}{r^2+h^2}$
Torsion of $\boldsymbol{P}(s)$	$\tau(s) = \frac{h}{r^2+h^2}$

effects of the orbital-like and the Zeeman-like contributions to the SOI. Such two contribution are both first order in the atomic carbon SOI constant for the π bands. And the orbital-like contribution can be understood as a "Rashba-type" SOI similar to graphene [47,48] and SCNTs [26,27], arising from the broken reflection symmetry, which is also the reason for the appearance of the Zeeman-like contribution. More interestingly, the asymmetric spin splitting, strikingly different from SCNTs, are shown to largely depend on the relevant parameters of HCCNTs (see Fig. 1). Our results well predict the modulation of asymmetric spin splitting by p and r for more than 320 HCCNTs within the tube diameter between 0.7 to 2.8 nm. In Fig. 1, $\boldsymbol{P}(s)$ is the position vector with the arc-length parameter s along the helical axis of HCCNTs. $\boldsymbol{T}(s)$, $\boldsymbol{N}(s)$ and $\boldsymbol{B}(s)$ are the tangent, normal and binormal vectors of $\boldsymbol{P}(s)$, respectively. Employing the formulas of $\kappa(s) = |\frac{d^2\boldsymbol{P}(s)}{ds^2}|$ and $\tau(s) = -\langle \boldsymbol{N}(s), \frac{d\boldsymbol{B}(s)}{ds}\rangle$, we can obtain the curvature $\kappa(s)$ and torsion $\tau(s)$ of $\boldsymbol{P}(s)$ for the central helical axis of HCCNT as listed in Table 1.

This paper is organized as follows. In Section 2, a brief introduction is given to the model and the details of calculation methods. Finally, we derive the effective SOI in HCCNTs. In Section 3, the effects of energy band splitting in the SOI strength for HCCNTs are described, and the results compared with that in SCNTs. In the last section, we present brief summary and conclusions.

2. Effective spin–orbit interaction in HCCNTs

The TB model has been well applied to graphene and SCNTs [25–27]. Considering the arbitrary atom of pentagon–heptagon pairs in HCCNTs is still surrounded by three nearest-neighbor atoms similar to the hexagon case, we reasonably choose this method in our calculations. The TB representation of Hamiltonian is defined by the combination of the contributions H_0 and H_{so},

$$H = H_0 + H_{so}. \tag{1}$$

The spin-independent noninteracting Hamiltonian reads $H_0 = \sum_{i\mu s} c_{is}^{\mu\dagger} t_i^{\mu} c_{is}^{\mu} + \sum_{\langle i\mu s, j\mu' s\rangle} c_{is}^{\mu\dagger} t_{i,j}^{\mu,\mu'} c_{js}^{\mu'}$, where $\langle i, j\rangle$ denotes neighboring atomic sites, the superscript $\langle \mu, \mu'\rangle$ for the s and p_x, p_y, p_z atomic orbitals on each site, the subscript $s = \uparrow, \downarrow$ for the electronic spin, and t_i^{μ} for the "on-site" atomic energies of $2s$ and $2p$ orbitals, i.e., the site-diagonal matrix elements t_i^s and t_i^p ($t_i^p = 0$). The strength of the hopping matrix element $t_{i,j}^{\mu,\mu'}$ is controlled by the effective overlap of neighboring atoms. Here we use one parameter V_{pp}^{π} for the nearest-neighbor hopping between the p_x orbitals of the π band, and other parameters of V_{pp}^{σ}, V_{sp}^{σ}, and V_{ss}^{σ} for the rest of the intra-atomic hoppings between the atomic orbitals s, p_y, p_z of the σ band. The SOI arises $H_{so}^{atom} = \frac{1}{2}\delta_{so}^{atom} \sum_i \mathbf{L}_i \cdot \mathbf{s}$ [49,50] with the atomic SOI constant δ_{so}^{atom}, the angular momentum operator $\mathbf{L}_i$ acting on the atomic orbitals at site i, and the electronic spin operator $\mathbf{s}$. The effect of this coupling is to mix single particle states with opposite spin from different orbitals, such as $c_{\uparrow}^{p_x}$ and $c_{\downarrow}^{p_y}$. Whether this leads to SOI in the band structure depends on how it affects hybridization between orbitals in different atoms, which in turn depends on the crystal structure. Besides, it should be stressed here that in our calculation, $\delta_{so}^{atom} = 6$ meV is used, which is estimated by the local spin density calculation for an isolated carbon atom in [26,48]. In fact, another different estimations of δ_{so}^{atom} have been done, e.g., $\delta_{so}^{atom} = 12$ meV in [23,25, 27,51,52], etc. However, the recent experiments of Ref. [22] point out an enhancement of the role of SOI in CNTs with respect to that of graphene; thus, the exact value of the SO coupling parameter is still under discussion.

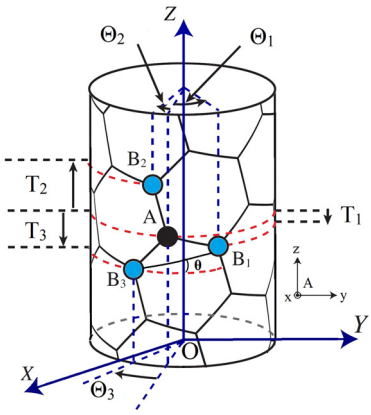

Fig. 2. (Color online.) A SCNT is defined by a rolled-up graphene sheet with chiral vector $n\mathbf{a}_1 + m\mathbf{a}_2 \equiv (n, m)$ and chiral angle $|\theta| \in [0, \pi/6]$. Both axis and circumference components of A to its nearest-neighbor three B atoms, (T_j, Θ_j) are shown with $T_j = -a_{CC}\gamma_j \cos(\theta + \delta_j)$ and $\Theta_j = a_{CC}\gamma_j \sin(\theta + \delta_j)$ ($\gamma_j = 1, -1, -1$ and $\delta_j = \pi/3, 0, 2\pi/3$). Surface coordinates are denoted by (x, y, z) which are defined at each atomic position, in which x is oriented normal to the surface, $y(z)$ tangent to the circumference (parallel to the nanotube axes). Three-dimensional coordinates are denoted by (X, Y, Z).

Following the approach in [23,26,27], we analyze the hopping between the neighboring atoms for the s, p_x, p_y and p_z orbitals in SCNTs (see Fig. 2). Here the p_x orbitals are oriented normal to the surface, the p_y orbitals tangent to the surface circumference, and the p_z orbitals parallel to the tube axes, which is different from the usual definition in [25,27] (i.e. p_z is normal to the surface). The curvature modifies the hopping for the $p_x(y)$ orbitals between the two neighboring compared to graphene, and we retain only the leading-order term in the expansion in terms of a_{CC}/D as follows,

$$\begin{aligned} H_h = \sum_i \sum_{j=1}^{3} \sum_{s=\uparrow,\downarrow} \big[& t_{i,j}^{s,p_x} \left(c_{is}^{p_x\dagger} c_{js}^{s} + c_{is}^{s\dagger} c_{js}^{p_x} \right) \\ & + t_{i,j}^{p_x,p_y} \left(c_{is}^{p_x\dagger} c_{js}^{p_y} - c_{is}^{p_y\dagger} c_{js}^{p_x} \right) \\ & + t_{i,j}^{p_x,p_z} \left(c_{is}^{p_x\dagger} c_{js}^{p_z} - c_{is}^{p_z\dagger} c_{js}^{p_x} \right) + t_{i,j}^{p_x,p_x} c_{is}^{p_x\dagger} c_{js}^{p_x} \big] + \text{H.c.}, \end{aligned} \tag{2}$$

where i is a lattice site in the sublattice A and its three nearest-neighbor sites j ($j = 1, 2, 3$) in the sublattice B. The expressions of